UCLA
Computational and Applied Mathematics

A Comprehensive Numerical Assessment, Implementation and Evaluation of a Constitutive Model Describing the Plastic Behavior of Metals During Phase Transformation, with Integration of Mixed Isotropic-Kinematic Strain Hardening

Koffi Enakoutsa
Yanni L. Bills

Department of Mathematics
University of California, Los Angeles
Los Angeles, CA, 90095-1555

Contents

List of Figures

List of Tables

1. ABSTRACT

This study meticulously explores the numerical implementation of Leblond *et al.*'s sophisticated model for phase transformation, concentrating on its application to crucial thermo-mechanical processes such as welding and quenching. The emphasis lies in assessing the precision and reliability of this implementation within finite element analysis, offering valuable insights into the intricate interplay of thermal, metallurgical, and mechanical phenomena. The practical applications of Leblond *et al.*'s model in predicting phase transformation phenomena in A.508cl. and A533 steels are showcased, underscoring its robustness and efficiency in providing accurate numerical simulations of thermo-mechanical processes. This research contributes significantly to advancing our understanding of material responses during phase transformations, thereby enhancing the predictive capabilities of computational tools in industrial applications.

2. INTRODUCTION

In thermo-mechanical processes like welding and quenching, prevalent in various industries, three key physical phenomena interact: thermal, metallurgical, and mechanical. To enable accurate numerical simulations of welding and quenching processes, it's essential to incorporate these thermal, metallurgical, and mechanical effects into computational codes. This ensures the development of robust numerical tools for predicting the behavior of industrial components undergoing these thermo-mechanical procedures. During these processes, thermal and mechanical actions cause phase transformations, leading to transformation deformations. In this study, the mechanical-induced phase changes are disregarded, attributing these phase changes solely to thermal effects, while simplifying certain aspects of the transformation process.

During thermal heating, steel undergoes austenization, transforming alpha iron into gamma iron. Subsequent cooling results in various transformations depending on the rate, with a focus on the γ austenite to α ferrite transformation in this study. These phase changes are driven by thermally and sometimes mechanically activated atomic network rearrangements, classified into two mechanisms: diffusive and displacive transformations. Diffusive transformations involve slower atom movements over longer distances, impacting atomic network compactness significantly, while displacive transformations are characterized by rapid atom displacements over shorter distances, distorting the crystalline structure into a metastable form. These phase transformations are primarily responsible for transformation deformations, predominantly due to volume changes, with the effects of shape changes disregarded for simplicity in this investigation.

During thermo-mechanical processes such as welding and quenching, which are widely used in industries, three main physical phenomena interact: thermal, metallurgical, and mechanical. In order to faithfully reproduce numerical simulations of welding processes (Inoue et al. [5]) and quenching processes (Inoue and Wang [6]), it is necessary to consider the thermal, metallurgical, and mechanical effects in the computational codes, making them robust tools for predicting the behavior of industrial components subjected to these thermo-mechanical processes.

During these processes, the thermal and mechanical operations induce phase transformations (Thermal and Mechanical $\rightarrow$ Metallurgical), which, in turn, result in a transformation deformation (Metallurgical $\rightarrow$ Mechanical). In this study, the phase changes induced by mechanical loading are neglected (Mechanical $\rightarrow$ Metallurgical). Therefore, these phase changes are solely due to thermal effects (Thermal $\rightarrow$ Metallurgical). Additionally, the thermal deformation (Thermal $\rightarrow$ Mechanical) will be considered isotropic, and intrinsic dissipation (Mechanical $\rightarrow$ Thermal) will not be taken into account, as it is considered negligible in relation to the studied phenomenon.

During a thermal heating process, steel undergoes austenization, meaning that

the α-iron (ferrite phase) transforms into γ-iron (austenite phase). During cooling, this austenite transforms into martensite, bainite, ferrite, perlite, or a mixture (α structure) depending on the cooling rate. This study focuses on the latter transformation (γ austenite $\rightarrow \alpha$ ferrite), which occurs during cooling. At the microscopic level, these phase changes result from rearrangements of thermally (and/or mechanically) activated atomic networks and are described by two mechanisms: displacive and diffusive. A phase change can be distinguished by these two types of transformations:

Diffusive transformations involve slow movements of atoms over long distances (greater than the interatomic distance) and generally occur at relatively slow cooling rates of the material. This diffusional transformation of carbon provides the time required for a stable rearrangement of carbon atoms. It is generally accompanied by a significant change in the atomic network's compactness. Consequently, the transformation deformation is predominantly dilatometric in nature in this transformation.

Displacive transformations involve rapid atom displacements over short distances (less than the inter-atomic distance) and generally occur at relatively high cooling rates. This non-diffusional transformation of carbon does not provide enough time for carbon atoms to move freely, resulting in a distorted crystalline structure. As a result, the transformation deformation has a dominant deviatoric component. These transformations are also referred to as shear transformations.

These phase transformations are responsible for the transformation deformations. In fact, the transformation deformation is mainly due to the change in shape and/or volume of different constituents (phases) during their transformations (Metallurgical $\rightarrow$ Mechanical). In this study, the effects of shape changes are neglected, and only the effects due to volume changes are considered, for reasons that will be discussed later.

The volume change arises from the difference in compactness between phases. The austenitic phase, with a compactness of 74%, has a face-centered cubic structure, while the ferritic phase, with a compactness of 68%, has a body-centered cubic structure.

These volume variations during phase transformations lead to changes in the mechanical behavior of structures. This is the primary motivation for developing mechanical models that can be integrated into finite element analysis software. These models aim to predict the behavior of these structures with the highest possible accuracy through numerical simulations of welding and quenching processes. These simulations include the evaluation of residual stresses and distortions that occur within the material during these thermo-mechanical processes.

One consequence of the transformation deformation resulting from thermo-mechanical interactions, as discussed in the previous section, is transformation

plasticity. Transformation plasticity occurs during thermo-mechanical treatments of steels and metallic alloys, such as quenching and welding, which induce residual stresses and material distortions, thereby altering their macroscopic mechanical behavior. It is commonly accepted that transformation plasticity is attributed to two primary mechanisms, one being diffusive (Greenwood and Johnson [4]) and the other being displacive (Magee and Paxton [9]).

The principle of Greenwood and Johnson [4] transformation plasticity mechanism lies in the plastic accommodation of the austenite phase (the softer phase) during the phase transformation. During cooling, the austenitic γ phase gives rise to a ferritic, bainitic, or martensitic α phase, which has a greater specific volume than its parent phase. When both phases coexist, the volume difference between them generates a field of heterogeneous deformation, resulting in internal stresses and macroscopic plastic flow, even if the macroscopic applied stress is below the yield strength of both phases or even zero. The first micro-mechanical model of this mechanism, established by Leblond *et al.* [7, 8], considers a representative spherical volume element of an expanding α phase core, surrounded by a concentric spherical shell of γ phase. When considering low macroscopic stresses, this approach leads to an expression for the rate of transformation plastic deformation that is linearly dependent on the deviatoric part of stresses.

To delve deeper into this subject, it is imperative to recognize that the behavior of metals during phase transformations is a critical aspect of materials engineering. Phase transformations can dramatically influence a material's properties, such as strength, ductility, and thermal conductivity, making them central to the design and performance of various engineering structures and components. The work hardening isotropic-kinematic model is particularly significant in this context because it offers a versatile and robust tool for characterizing and predicting the mechanical response of materials as they undergo phase transformations. It encompasses both isotropic hardening, which accounts for the evolution of the yield stress with deformation, and kinematic hardening, which considers the evolution of the material's anisotropy.

Moreover, the integration of this model within the finite element analysis (FEA) framework is a pivotal development. When applied to phase transformations in metals, FEA combined with the mixed work hardening isotropic-kinematic model enables to gain insights into the deformation and stress distribution within materials as they undergo phase changes. This can facilitate the optimization of material selection and the design of components with enhanced performance and durability.

This opportunity will be taken to simplify and rationalize the numerical implementation of this behavior for the other types of hardening (namely, ideal perfect plasticity, isotropic hardening, kinematic hardening). First, in fact, this numerical implementation presents some unnecessary complications, such as the use sometimes of a semi-implicit algorithm whereas a totally explicit, much simpler, algorithm does not lead to a significant degradation of the precision. Second, various

additional effects have been introduced into the modeling (for example, restoration or the memory of work hardening during transformations, effect of large transformations, etc.), their numerical implementation not always being carried out in the same mind than the initial numerical implementation (usually for the sake of simplicity). A general "grooming" therefore seems desirable.

Some new needs have recently appeared concerning the possibility of a mixed work hardening isotropic-kinematic in the modeling of the plastic behavior of metals during phase transformation developed by Leblond *et al.* [7, 8]. The objective of this note is to describe without insisting on the theoretical aspects, such a modeling, as well as its numerical implementation within the framework of the finite element element analysis of phase transformations in metals.

The remainder of the paper unfolds in the subsequent sections as follows:

1. In Section 1, a comprehensive overview of the constitutive equations proposed by Leblond *et al.* [7, 8] is presented, outlining their constitutive model for phase transformation.
2. Moving forward to Section 2, a detailed account of the numerical implementation of this model into a finite element code is provided.
3. Finally, Section 3 showcases the practical application of the model by presenting numerical predictions for a phase transformation scenario involving A.508cl. and A533 steels. The obtained results not only affirm the robustness of the implemented numerical framework but also underscore the model's efficiency in accurately predicting phase transformation phenomena in steels.

.

3. THERMO-PLASTICITY BEHAVIOR FOR A MIXED ISOTROPIC-KINEMATIC HARDENING.

Let us begin for the sake of completeness by recalling the model of plastic behavior with mixed work hardening used in the standard finite element codes, in the absence of phase transformation. We consider the general case of a variable temperature and large deformations.

Let $\sigma_0(T)$ be the initial limit of elasticity, before work hardening, function only of the temperature$T$. Let $\sigma(\varepsilon_{eq}, T)$ be the stress observed in an initial tensile test at the temperature T, function of this temperature and of the cumulated plastic deformation ε_{eq}. Let

$$\overline{\sigma}(\varepsilon_{eq}, T) \equiv \sigma(\varepsilon_{eq}, T) - \sigma_0(T) \tag{1}$$

the part of this stress coming from work hardening. Finally, let p be the proportion

of work hardening which is of an isotropic nature.

The limit of elasticity is therefore

$$\sigma^Y(\varepsilon_{eq}, T) \equiv \sigma_0(T) + p\overline{\sigma}(\varepsilon_{eq}, T) \tag{2}$$

The yield criterion is then written as

$$\sigma_{eq} \equiv \left[\frac{3}{2}(\underline{\underline{s}} - \underline{\underline{a}}) : (\underline{\underline{s}} - \underline{\underline{a}})\right]^{\frac{1}{2}} \leq \sigma^Y(\varepsilon_{eq}, T) \tag{3}$$

where $\underline{\underline{s}}$ denotes the deviatoric stress. The evolution equation of the center $\underline{\underline{a}}$ of the domain of elasticity is:

$$\overset{\circ}{\underline{\underline{a}}} \equiv \dot{\underline{\underline{a}}} + \left(\dot{\underline{\underline{a}}}\right)_{GT} = \frac{2}{3}(1-p)\frac{\partial\overline{\sigma}}{\partial\varepsilon_{eq}}(\varepsilon_{eq}, T)\underline{\underline{d}}^p + \frac{1}{\overline{\sigma}}\frac{\partial\overline{\sigma}}{\partial T}(\varepsilon_{eq}, T)\underline{\underline{a}}\dot{T} \tag{4}$$

In this equation, $\overset{\circ}{\underline{\underline{a}}}$ denotes the objective derivative of a chosen (for example, those of Jaumann or Molinari) and $\left(\dot{\underline{\underline{a}}}\right)_{GT}$ the part, in the expression of this objective derivative, due to large deformations. In addition, $\underline{\underline{d}}^p$ denotes the plastic strain rate (Eulerian). Finally, for the record, the plastic constitutive law is the same as usual.

$$\underline{\underline{d}}^p = \frac{3}{2}\frac{\dot{\varepsilon_{eq}}}{\sigma_{eq}}(\underline{\underline{s}} - \underline{\underline{a}}), \qquad \dot{\varepsilon}_{eq} = \left(\frac{2}{3}\underline{\underline{d}}^p : \underline{\underline{d}}^p\right)^{\frac{1}{2}} \tag{5}$$

4. PLASTIC BEHAVIOR DURING PHASE TRANSFORMATION IN THE CASE OF MIXED ISOTROPIC-KINEMATIC HARDENING

We will not include here the details to the homogenization approach leading to the macroscopic equations of plastic behavior during phase transformations. Details on this derivation can be found in the works of Leblond *et al.* [7, 8] We will only indicate the results, within the framework of a mixed isotropic-kinematic hardening.

4.1. Generalities

The parent-phase (γ) is denoted with an index of 1, and the daughter-phase α with an index of 2; z denotes the proportion of daughter-phase ($\dot{z}$). We denote $\overline{\sigma}_i(\varepsilon_i^{\mathit{eff}}, T)$ the part coming from the work hardening in the stress observed in a simple tensile test, carried out on a sample of pure phase i. This quantity is a function of the effective plastic strain eff of the phase i, which may differ from the equivalent strain due to the phenomena of memory and restoration of work hardening during the transformations. We denote $\sigma_i^Y(\varepsilon_i^{\mathit{eff}}, T)$ the limit of elasticity of phase i, given

by a formula analogous to Eq.2 (with σ_i^0 and $\overline{\sigma}_i$ instead of $\overline{\sigma}_i$ and σ_0). We denote $\underline{\underline{a}}_i$ the center of the elasticity domain of phase i.

Finally, the overall limit stress is given by the formula.

$$\sigma^Y(\varepsilon_1^{eff}, \varepsilon_2^{eff}, z, T) = [1 - f(z)]\sigma_1^Y(\varepsilon_1^{eff}, T) + f(z)\sigma_2^Y(\varepsilon_2^{eff}, T) \tag{6}$$

4.2. Case where the stress is less than the yield limit

This case is defined by the condition

$$\sigma_{eq} < \sigma^Y, \quad \sigma_{eq} \equiv \left[\frac{3}{2}(\underline{\underline{s}} - \underline{\underline{a}}) : (\underline{\underline{s}} - \underline{\underline{a}})\right]^{\frac{1}{2}}, \quad \underline{\underline{a}} \equiv (1-z)\underline{\underline{a}}_1 + z\underline{\underline{a}}_2 \tag{7}$$

The other part of the plastic strain rate corresponding to the plasticity of transformation is written as

$$\underline{\underline{d}}^{pt} = -3\frac{\varepsilon_2^{th}(T) - \varepsilon_1^{th}(T)}{\sigma_1^Y(\varepsilon_1^{eff}, T)} h\left(\frac{\sigma_{eq}}{\sigma^Y}\right)(\ln z)(\underline{\underline{s}} - \underline{\underline{a}}_1)\dot{z} \tag{8}$$

where $\varepsilon_i^{th}(T)$ is the thermal deformation of the phase i. The part of the rate of plastic deformation corresponding to the plastic plasticity is decomposed into 2 terms, one, $\underline{\underline{d}}_{\sigma}^{pc}$ coming from the variations of $\underline{\underline{\sigma}}$ and the other, $\underline{\underline{d}}_{T}^{pc}$, coming from the variations of T is given by

$$\underline{\underline{d}}_{\sigma}^{pc} = \frac{3}{2}\frac{1-z}{\sigma_1^Y(\varepsilon_1^{eff}, T)}\frac{g(z)}{E}(\underline{\underline{s}} - \underline{\underline{a}}_1)(\dot{\sigma}_1^{eq})_s \tag{9}$$

$$(\dot{\sigma}_1^{eq})_s \equiv \frac{3}{2\sigma_1^{eq}}(\underline{\underline{s}} - \underline{\underline{a}}_1) : \overset{\circ}{\underline{\underline{s}}}, \quad \sigma_1^{eq} \equiv \left[\frac{3}{2}(\underline{\underline{s}} - \underline{\underline{a}}_1) : (\underline{\underline{s}} - \underline{\underline{a}}_1)\right]^{\frac{1}{2}} \tag{10}$$

$$\underline{\underline{d}}_{T}^{pc} = 3\frac{\alpha_1 - \alpha_2}{\sigma_1^Y(\varepsilon_1^{eff}, T)} z(\ln z)(\underline{\underline{s}} - \underline{\underline{a}}_1)\dot{T} \tag{11}$$

where α_i denotes the coefficient of the thermal dilatation of the phase i.

The evolution equations of the effective plastic deformation of the phases are as follow

$$\dot{\varepsilon}_1^{eff} = -2\frac{\varepsilon_1^{th}(T) - \varepsilon_2^{th}(T)}{1-z} h\left(\frac{\sigma_{eq}}{\sigma^Y}\right)(\ln z)\dot{z} + \frac{g(z)}{E}(\dot{\sigma}_1^{eq})_s + 2\frac{\alpha_1 - \alpha_2}{1-z} z(\ln z)\dot{T} \tag{12}$$

$$\dot{\varepsilon}_2^{eff} = \frac{\dot{z}}{z}\varepsilon_2^{eff} + \theta\frac{\dot{z}}{z}\dot{\varepsilon}_1^{eff} \tag{13}$$

where θ denotes the memory coefficient of the work hardening during the transformation ($\theta = 0$ means that the hardening of the mother-phase is completely forgotten by the daughter-phase during the transformation, $\theta = 1$, that this work hardening is, on the contrary, entirely transferred to the daughter-phase.) Finally, the evolution equations of the centers of the elasticity domain of the phases are as follows:

$$\overset{\circ}{\underline{\underline{a}}}_1 \equiv \dot{\underline{\underline{a}}}_1 + (\dot{\underline{\underline{a}}}_1)_{GT} = \frac{2}{3}\frac{1-p}{1-z}\frac{\partial\overline{\sigma_1}}{\partial\varepsilon_1^{eff}}(\varepsilon_1^{eff},T)(\underline{\underline{d}}^{pt} + \underline{\underline{d}}_{\sigma}^{pc} + \underline{\underline{d}}_{T}^{pc}) + \frac{1}{\overline{\sigma}_1}\frac{\partial\overline{\sigma_1}}{\partial T}(\varepsilon_1^{eff},T)\underline{\underline{a}}_1\dot{T} \tag{14}$$

$$\overset{\circ}{\underline{\underline{a}}}_2 \equiv \dot{\underline{\underline{a}}}_2 + (\dot{\underline{\underline{a}}}_2)_{GT} = -\frac{\dot{z}}{z}\underline{\underline{a}}_2 + \theta\frac{\dot{z}}{z}\underline{\underline{a}}_1 + \frac{1}{\overline{\sigma}_2}\frac{\partial\overline{\sigma_2}}{\partial T}(\varepsilon_2^{eff},T)\underline{\underline{a}}_2\dot{T} \tag{15}$$

4.3. Case where the stress equals the yield limit

This case is defined by the condition

$$\sigma_{eq} = \sigma^Y \tag{16}$$

where σ_{eq} is always defined by by the relations Eq.(7). The flow rule is then

$$\underline{\underline{d}}^p = \frac{3}{2}\frac{\dot{\varepsilon}_{eq}}{\sigma_{eq}}(\underline{\underline{s}} - \underline{\underline{a}}) \qquad (\text{with } \dot{\varepsilon}_{eq} = \left(\frac{2}{3}\underline{\underline{d}}_p : \underline{\underline{d}}_p\right)^{\frac{1}{2}}) \tag{17}$$

The evolution equations of the work hardening are written as follows:

$$\dot{\varepsilon}_1^{eff} = \dot{\varepsilon}_{eq} \tag{18}$$

$$\dot{\varepsilon}_2^{eff} = \dot{\varepsilon}_{eq} - \frac{\dot{z}}{z}\varepsilon_2^{eff} + \theta\frac{\dot{z}}{z}\dot{\varepsilon}_1^{eff} \tag{19}$$

$$\overset{\circ}{\underline{\underline{a}}}_1 = \frac{2}{3}(1-p)\frac{\partial\overline{\sigma_1}}{\partial\varepsilon_1^{eff}}(\varepsilon_1^{eff},T)\underline{\underline{d}}^p + \frac{1}{\overline{\sigma}_1}\frac{\partial\overline{\sigma_1}}{\partial T}(\varepsilon_1^{eff},T)\underline{\underline{a}}_1\dot{T} \tag{20}$$

$$\overset{\circ}{\underline{\underline{a}}}_2 = \frac{2}{3}(1-p)\frac{\partial\overline{\sigma_2}}{\partial\varepsilon_2^{eff}}(\varepsilon_2^{eff},T)\underline{\underline{d}}^p + \frac{1}{\overline{\sigma}_2}\frac{\partial\overline{\sigma_2}}{\partial T}(\varepsilon_2^{eff},T)\underline{\underline{a}}_2\dot{T} - \frac{\dot{z}}{z}\underline{\underline{a}}_2 + \theta\frac{\dot{z}}{z}\underline{\underline{a}}_1 \tag{21}$$

5. NUMERICAL IMPLEMENTATION

About each equation arises the problem of the choice of the algorithm: explicit, implicit, semi implicit. The choices made here, which do not coincide exactly with the previous choice, are dictated by the following considerations.

a. An explicit algorithm is preferable if it makes it possible to simplify the digitization without significantly degrading its accuracy;
b. an implicit algorithm is preferable with respect to the direction of the plastic flow (given by the stress deviator) for the sake of consistency with the standard programming in finite element codes;
c. a semi-implicit algorithm is preferable if it significantly improves accuracy, or if, even if it doesn't, it doesn't significantly complicate the numerization.

5.1. Case where the yield limit is not reached

The partition of the deviator of the increment of the total strain (thermal part substracted) between the times t and $t+\Delta t$ is written as

$$\Delta \underline{\underline{e}} = \Delta \underline{\underline{e}}^e + \Delta \underline{\underline{\varepsilon}}^p = \Delta \underline{\underline{e}}^e + (\Delta \underline{\underline{\varepsilon}}^p)' + (\Delta \underline{\underline{\varepsilon}}^p)'' \tag{22}$$

where the term $\left((\Delta \underline{\underline{\varepsilon}}^p)'\right)$ corresponds to $\left(\underline{\underline{d}}_{pt} + \underline{\underline{d}}^{pc}_{T}\right)\Delta t$ and $\left((\Delta \underline{\underline{\varepsilon}}^p)''\right)$ to $\left(\underline{\underline{d}}^{pc}_{\sigma}\right)\Delta t$. The expressions of these terms are the following, where F denotes the function of the von Mises $\left(F(\underline{\underline{X}}) = \left(\frac{3}{2}\underline{\underline{X}} : \underline{\underline{X}}\right)^{1/2}\right)$:

$$(\Delta \underline{\underline{\varepsilon}}^p)' = \frac{A}{2}\left[1 + \frac{F(\underline{\underline{s}} - \underline{\underline{a}}_1)}{F(\underline{\underline{s}} + \Delta\underline{\underline{s}} - \underline{\underline{a}}_1 - \Delta\underline{\underline{a}}_1)}\right](\underline{\underline{s}} + \Delta\underline{\underline{s}} - \underline{\underline{a}}_1 - \Delta\underline{\underline{a}}_1) \tag{23}$$

$$(\Delta \underline{\underline{\varepsilon}}^p)'' = \frac{B}{2}\left[1 + \frac{F(\underline{\underline{s}} - \underline{\underline{a}}_1)}{F(\underline{\underline{s}} + \Delta\underline{\underline{s}} - \underline{\underline{a}}_1 - \Delta\underline{\underline{a}}_1)}\right](\Delta\sigma_1^{eq})_s(\underline{\underline{s}} + \Delta\underline{\underline{s}} - \underline{\underline{a}}_1 - \Delta\underline{\underline{a}}_1) \tag{24}$$

In the expression Eq.(23), A is given by

$$A = -3\frac{\varepsilon_2^{th}(T) - \varepsilon_1^{th}(T) + \varepsilon_2^{th}(T+\Delta T) - \varepsilon_1^{th}(T+\Delta T)}{\sigma_1^Y(\varepsilon_1^{\mathit{eff}}, T) + \sigma_1^Y(\varepsilon_1^{\mathit{eff}}, T+\Delta T)} h\left(\frac{\sigma_{eq}}{\sigma^Y}\right)\{(z+\Delta z)[\ln(z+\Delta z) - 1] - z(\ln z - 1)\}$$
$$+ 3\frac{\varepsilon_1^{th}(T+\Delta T) - \varepsilon_1^{th}(T) + \varepsilon_2^{th}(T+\Delta T) - \varepsilon_2^{th}(T)}{\sigma_1^Y(\varepsilon_1^{\mathit{eff}}, T) + \sigma_1^Y(\varepsilon_1^{\mathit{eff}}, T+\Delta T)}[z\ln z + (z+\Delta Z)\ln(z+\Delta z)] \tag{25}$$

The term $h(\sigma_{eq}\overline{/}\sigma^Y)$ in this expression is discretized explicitly. Moreover, the term comes from an exact integration of $\ln(z)$ between z and $z+\Delta z$ in Eq.(8), the other

terms being considered constant. Numerical experiments have shown the importance of such exact integration to conveniently reproduce stress dilatometry tests.

The quantity B in Eq.(24) is given by

$$B = 3\frac{(1-z)g(z) + (1-z-\Delta z)g(z+\Delta z)}{\left[\sigma_1^Y(\varepsilon_1^{eff}, T) + \sigma_1^Y(\varepsilon_1^{eff}, T+\Delta T)\right][E(T) + E(T+\Delta T)]} \tag{26}$$

In addition, $(\Delta\sigma_1^{eq})_s$, is given by

$$(\Delta\sigma_1^{eq})_s = \frac{3}{2F(\underline{\underline{s}} + \Delta\underline{\underline{s}} - \underline{\underline{a}}_1 - \Delta\underline{\underline{a}}_1)}(\underline{\underline{s}} + \Delta\underline{\underline{s}} - \underline{\underline{a}}_1 - \Delta\underline{\underline{a}}_1) : (\Delta\underline{\underline{s}})_{OBJ} \tag{27}$$

where $(\Delta\underline{\underline{s}})_{OBJ}\left(\equiv \check{\underline{\underline{s}}}\right)$ is the objective part of the deviatoric stress rate

$$(\Delta\underline{\underline{s}})_{OBJ} \equiv \Delta\underline{\underline{s}} + (\Delta\underline{\underline{s}})_{GT} \tag{28}$$

The hypo-elasticity law is given by

$$(\Delta\underline{\underline{s}})_{OBJ}(= \Delta\underline{\underline{s}} + (\Delta\underline{\underline{s}})_{GT}) = 2\mu\Delta\underline{\underline{e}}^e + (\Delta\underline{\underline{s}})_T \tag{29}$$

where μ denotes the shear coefficient at the time $t+\Delta t$ (this notation is used here rather than the more logical notation $\mu + \Delta\mu$ to simplify the writing) and $(\Delta\underline{\underline{s}})_T$ the part of $\Delta\underline{\underline{s}}$ coming from the variation of the temperature (via its influence on μ.) The evolution equation of ε_1^{eff} is discretized as the following equation:

$$\Delta\varepsilon_1^{eff} = \frac{2}{3}\frac{\sigma_1^Y(\varepsilon_1^{eff}, T) + \sigma_1^Y(\varepsilon_1^{eff}, T+\Delta T)}{(1-z) + (1-z+\Delta z)}[A + B(\Delta\sigma_1^{eq})_s] \tag{30}$$

The equation of ε_1^{eff} is written in the form $\frac{d}{dt}\left(0z\varepsilon_1^{eff}\right) = \theta\varepsilon_1^{eff}\dot{z}$ before being discrtized by

$$\Delta(z\varepsilon_2^{eff}) \equiv (z+\Delta z)(\varepsilon_2^{eff} + \Delta\varepsilon_2^{eff}) - z\varepsilon_2^{eff} = \theta\varepsilon_1^{eff}\Delta z \tag{31}$$

Similarly, the evolution equations of $\underline{\underline{a}}_1$ and $\underline{\underline{a}}_2$ are discretized as follows:

$$\begin{aligned}
&(\Delta\underline{\underline{a}}_1)_{OBJ} \equiv \Delta\underline{\underline{a}}_1 + (\Delta\underline{\underline{a}}_1)_{GT} = \frac{2}{3}\frac{1-p}{1-z-\Delta z/2}\frac{\partial\overline{\sigma}_1}{\partial\varepsilon_1^{eff}}(\varepsilon_1^{eff}, T+\Delta T)\\
&\left[(\Delta\underline{\underline{\varepsilon}}^p)' + \varepsilon^p)''\right] + (\Delta\underline{\underline{a}}_1)_T\\
&\implies \Delta\underline{\underline{a}}_1 = \frac{2}{3}\frac{1-p}{1-z-\Delta z/2}\frac{\partial\overline{\sigma}_1}{\partial\varepsilon_1^{eff}}(\varepsilon_1^{eff}, T+\Delta T)\left[(\Delta\underline{\underline{\varepsilon}}^p)' + (\Delta\underline{\underline{\varepsilon}}^p)''\right]\\
&- (\Delta\underline{\underline{a}}_1)_{GT} + (\Delta\underline{\underline{a}}_1)_T
\end{aligned} \tag{32}$$

Note in Eq.(32) the use of the hardening slope $\frac{\partial\overline{\sigma}_1}{\partial\varepsilon_1^{\mathit{eff}}}(\varepsilon_1^{\mathit{eff}}, T+\Delta T)$ instead of the secant as previously. The interest of this replacement is to lead to an explicit resolution not requiring iterations on the parameter of work hardening $\varepsilon_1^{\mathit{eff}} + \Delta\varepsilon_1^{\mathit{eff}}$; it is licit insofar as there are no criteria to be satisfied exactly at the time $t+\Delta t$ (it will not be the same if the yield limit is reached.) Moreover, note that the terms $(\Delta\underline{\underline{a}}_i)_{GT}$ and $(\Delta\underline{\underline{a}}_i)_T$ are discretized in an explicit way and therefore known from the beginning.

Now let us move on to solving these equations; the principal unkowns used are

$$\Delta(z\underline{\underline{a}}_2) \equiv (z+\Delta z)(\underline{\underline{a}}_2 + \Delta\underline{\underline{a}}_2) - z\underline{\underline{a}}_2 = \theta\underline{\underline{a}}_1\Delta z - z(\Delta\underline{\underline{a}}_2)_{GT} + z(\Delta\underline{\underline{a}}_2)_T \tag{33}$$

Combining Eq.(22) and Eq.(29) we get

$$X = F(\underline{\underline{s}} + \Delta\underline{\underline{s}} - \underline{\underline{a}}_1 - \Delta\underline{\underline{a}}_1), \quad Y = (\Delta\sigma_1^{eq})_s \tag{34}$$

$$\begin{aligned} &\Delta\underline{\underline{s}} = 2\mu\Delta\underline{\underline{e}}^e - (\Delta\underline{\underline{s}})_{GT} + (\Delta\underline{\underline{s}})_T \quad \Longrightarrow \\ &\underline{\underline{s}} + \Delta\underline{\underline{s}} \equiv (\underline{\underline{s}} + \Delta\underline{\underline{s}})^{el} - 2\mu\left[(\Delta\underline{\underline{\varepsilon}}^p)' + (\Delta\underline{\underline{\varepsilon}}^p)''\right] \end{aligned} \tag{35}$$

$$(\underline{\underline{s}} + \Delta\underline{\underline{s}})^{el} \equiv \underline{\underline{s}} + 2\mu\Delta\underline{\underline{e}} - (\Delta\underline{\underline{s}})_{GT} + (\Delta\underline{\underline{s}})_T \tag{36}$$

where $(\underline{\underline{s}} + \Delta\underline{\underline{s}})^{el}$, known quantity, is the deviatoric stress at $t+\Delta t$ elastically calculted, that is by considering the deviatoric part of the increment of the total strain $\Delta\underline{\underline{e}}$ (with the termal part not being accounted for) as purely elastic. Adding $-\underline{\underline{a}}_1 - \Delta\underline{\underline{a}}_1$ to the two sides of Eq.(35) and taking into account Eq.(32), we get

$$\begin{aligned} \underline{\underline{s}} + \Delta\underline{\underline{s}} - \underline{\underline{a}}_1 - \Delta\underline{\underline{a}}_1 &= (\underline{\underline{s}} + \Delta\underline{\underline{s}})^{el} - \underline{\underline{a}}_1 - \Delta\underline{\underline{a}}_1 - 2\mu\left[(\Delta\underline{\underline{\varepsilon}}^p)' + (\Delta\underline{\underline{\varepsilon}}^p)''\right] \\ &= (\underline{\underline{s}} + \Delta\underline{\underline{s}})^{el} - \underline{\underline{a}}_1 + (\Delta\underline{\underline{a}}_1)_{GT} - (\Delta\underline{\underline{a}}_1)_T \\ &\quad - \left[2\mu + \frac{2}{3}\frac{1-p}{1-z-\Delta z/2}\frac{\partial\overline{\sigma}_1}{\partial\varepsilon_1^{\mathit{eff}}}(\varepsilon_1^{\mathit{eff}}, T+\Delta T)\right]\left[(\Delta\underline{\underline{\varepsilon}}^p)' + (\Delta\underline{\underline{\varepsilon}}^p)''\right] \end{aligned}$$

which, by setting

$$\underline{\underline{s}}^* \equiv (\underline{\underline{s}} + \Delta\underline{\underline{s}})^{el} - \underline{\underline{a}}_1 + (\Delta\underline{\underline{a}}_1)_{GT} - (\Delta\underline{\underline{a}}_1)_T \tag{37}$$

is equivalent to

$$H \equiv \frac{1-p}{1-z-\Delta z/2}\frac{\partial\overline{\sigma}_1}{\partial\varepsilon_1^{\mathit{eff}}}(\varepsilon_1^{\mathit{eff}}, T+\Delta T) \tag{38}$$

(these quantities are known):

$$\underline{\underline{s}} + \Delta\underline{\underline{s}} - \underline{\underline{a}}_1 - \Delta\underline{\underline{a}}_1 = \underline{\underline{s}}^* - 2\left(\mu + \frac{H}{3}\right)\left[(\Delta\underline{\underline{\varepsilon}}^p)' + (\Delta\underline{\underline{\varepsilon}}^p)''\right]$$

According to Eq.(23) and Eq.(24) and the notations Eq.(34) we get

$$(\Delta\underline{\underline{\varepsilon}}^p)' + (\Delta\underline{\underline{\varepsilon}}^p)'' = \frac{1}{2}(A+BY)\left(1+\frac{F(\underline{\underline{s}}-\underline{\underline{a}}_1)}{X}\right)(\underline{\underline{s}}+\Delta\underline{\underline{s}}-\underline{\underline{a}}_1-\Delta\underline{\underline{a}}_1) \tag{39}$$

which by reporting in the previous equation reads

$$\begin{aligned}
&\underline{\underline{s}}+\Delta\underline{\underline{s}}-\underline{\underline{a}}_1-\Delta\underline{\underline{a}}_1 = \underline{\underline{s}}^* - \left(\mu+\frac{H}{3}\right)(A+BY)\left(1+\frac{F(\underline{\underline{s}}-\underline{\underline{a}}_1)}{X}\right)(\underline{\underline{s}}+\Delta\underline{\underline{s}}-\underline{\underline{a}}_1-\Delta\underline{\underline{a}}_1)\\
&\Rightarrow \left[1+\left(\mu+\frac{H}{3}\right)(A+BY)\left(1+\frac{F(\underline{\underline{s}}-\underline{\underline{a}}_1)}{X}\right)\right](\underline{\underline{s}}+\Delta\underline{\underline{s}}-\underline{\underline{a}}_1-\Delta\underline{\underline{a}}_1) = \underline{\underline{s}}^*
\end{aligned} \tag{40}$$

This equation implies that the (unknown) tensor $\underline{\underline{s}}+\Delta\underline{\underline{s}}-\underline{\underline{a}}_1-\Delta\underline{\underline{a}}_1$ is positively parallel to the (unknown) tensor $\underline{\underline{s}}^*$. Thus,

$$\underline{\underline{s}}+\Delta\underline{\underline{s}}-\underline{\underline{a}}_1-\Delta\underline{\underline{a}}_1 = \frac{X}{F(\underline{\underline{s}}^*)}\underline{\underline{s}}^* \tag{41}$$

which brings the calculation of the unknown $\underline{\underline{s}}+\Delta\underline{\underline{s}}-\underline{\underline{a}}_1-\Delta\underline{\underline{a}}_1$ to the same of the norm of X. Moreover, by taking the Von Mises function of Eq.(41), we obtain:

$$\begin{aligned}
&X+\left(\mu+\frac{H}{3}\right)(A+BY)\left(X+F(\underline{\underline{s}}-\underline{\underline{a}}_1)\right) = F(\underline{\underline{s}}^*)\\
&\Rightarrow A+BY = \frac{F(\underline{\underline{s}}^*)-X}{\left(\mu+\frac{H}{3}\right)\left(X+F(\underline{\underline{s}}-\underline{\underline{a}}_1)\right)}\\
&\Leftrightarrow Y = \frac{1}{B}\left[\frac{F(\underline{\underline{s}}^*)-X}{\left(\mu+\frac{H}{3}\right)\left(X+F(\underline{\underline{s}}-\underline{\underline{a}}_1)\right)}-A\right]
\end{aligned} \tag{42}$$

The unknown quantity Y can now be expressed as a function of the unknown X, it remains to calculate the latter. For this, let us re-express $\underline{\underline{s}}+\Delta\underline{\underline{s}}-\underline{\underline{a}}_1-\Delta\underline{\underline{a}}_1$ using the equations Eq. 28 and Eq.(28) and Eq. (30) as well as the definition Eq. (38) as:

$$\underline{\underline{s}}+\Delta\underline{\underline{s}}-\underline{\underline{a}}_1-\Delta\underline{\underline{a}}_1 = \underline{\underline{s}}-(\Delta\underline{\underline{s}})_{GT}+(\Delta\underline{\underline{s}})_{OBJ}-\underline{\underline{a}}_1-\frac{2}{3}H\left[(\Delta\underline{\underline{\varepsilon}}^p)'+(\Delta\underline{\underline{\varepsilon}}^p)''\right]+(\Delta\underline{\underline{a}}_1)_{GT}-(\Delta\underline{\underline{a}}_1)_T$$

which, by accounting for Eq.39 and Eq. 42, reads

$$\begin{aligned}
\underline{\underline{s}}+\Delta\underline{\underline{s}}-\underline{\underline{a}}_1-\Delta\underline{\underline{a}}_1 &= \underline{\underline{s}}-(\Delta\underline{\underline{s}})_{GT}-\underline{\underline{a}}_1+(\Delta\underline{\underline{a}}_1)_{GT}-(\Delta\underline{\underline{a}}_1)_T\\
&\quad-\frac{H}{3}(A+BY)\left(1+\frac{F(\underline{\underline{s}}-\underline{\underline{a}}_1)}{X}\right)(\underline{\underline{s}}+\Delta\underline{\underline{s}}-\underline{\underline{a}}_1-\Delta\underline{\underline{a}}_1)+(\Delta\underline{\underline{s}})_{OBJ}\\
&= \underline{\underline{s}}-(\Delta\underline{\underline{s}})_{GT}-\underline{\underline{a}}_1+(\Delta\underline{\underline{a}}_1)_{GT}-(\Delta\underline{\underline{a}}_1)_T\\
&\quad+\frac{H\left(X-F(\underline{\underline{s}}^*)\right)}{(H+3\mu)\left(X+F(\underline{\underline{s}}-\underline{\underline{a}}_1)\right)}\left(1+\frac{F(\underline{\underline{s}}-\underline{\underline{a}}_1)}{X}\right)(\underline{\underline{s}}+\Delta\underline{\underline{s}}-\underline{\underline{a}}_1-\Delta\underline{\underline{a}}_1)+(\Delta\underline{\underline{s}})_{OBJ}
\end{aligned}$$

Contracting this equation with $\frac{3}{2}\underline{\underline{s}}^*$ gives, taking into account the definition Eq.(27) of $\left(\Delta\sigma_1^{eq}\right)_s \equiv Y$ and the property Eq.(41)

$$XF(\underline{\underline{s}}^*) = P + \frac{H\left(X - F(\underline{\underline{s}}^*)\right)}{(H+3\mu)\left(X + F(\underline{\underline{s}} - \underline{\underline{a}}_1)\right)}\left(X + F(\underline{\underline{s}} - \underline{\underline{a}}_1)\right)F(\underline{\underline{s}}^*) + F(\underline{\underline{s}}^*)Y$$

where we assumed that

$$P \equiv \frac{3}{2}\left(\underline{\underline{s}} - (\Delta\underline{\underline{s}})_{GT} - \underline{\underline{a}}_1 + (\Delta\underline{\underline{a}}_1)_{GT} - (\Delta\underline{\underline{a}}_1)_T\right) : \underline{\underline{s}}^*$$

(P is a known quantity). Multiplying by $(H+3\mu)\left(X + F(\underline{\underline{s}} - \underline{\underline{a}}_1)\right)$ and accounting for Eq.(42)

$$\begin{aligned}
&(H+3\mu)\left(X + F(\underline{\underline{s}} - \underline{\underline{a}}_1)\right)XF(\underline{\underline{s}}^*) = P(H+3\mu)\left(X + F(\underline{\underline{s}} - \underline{\underline{a}}_1)\right)\\
&+ H\left(X - F(\underline{\underline{s}}^*)\right)\left(X + F(\underline{\underline{s}} - \underline{\underline{a}}_1)\right)F(\underline{\underline{s}}^*)\\
&+ \frac{F(\underline{\underline{s}}^*)}{B}\left[3\left(F(\underline{\underline{s}}^*) - X\right) - A(H+3\mu)\left(X + F(\underline{\underline{s}} - \underline{\underline{a}}_1)\right)\right]
\end{aligned}$$

which gives after multiplication by B and re-arrangment:

Equation 43 is missing (43)

$$LX^2 + MX + N = 0 \tag{44}$$

$$L \equiv 3\mu BF(\underline{\underline{s}}^*) \tag{45}$$

$$M \equiv 3\mu BF(\underline{\underline{s}} - \underline{\underline{a}}_1)F(\underline{\underline{s}}^*) + BHF^2(\underline{\underline{s}}^*) + A(H+3\mu)F(\underline{\underline{s}}^*) - B(H+3\mu)P \tag{46}$$

The roots of this equation are $\frac{1}{2L}\left(-M \pm \sqrt{M^2 - 4LN}\right)$. The choice of the sign in front of the radical is not obvious a priori because as much as it is clear that $L > 0$, M and N can a priori take any sign. However, in practice, the coefficient B is small. We then see from Eq.(46) that $M > 0$, the $-$ sign in front of the radical then leads to a negative root, which is impossible since the equation is greater than $X \equiv F\left(\underline{\underline{s}} + \Delta\underline{\underline{s}} - \underline{\underline{a}}_1 - \Delta\underline{\underline{a}}_1\,()\right) > 0$, therefore the $+$ sign that must be retained.

$$N \equiv -3F^2(\underline{\underline{s}}^*) + BHF(\underline{\underline{s}} - \underline{\underline{a}}_1)F^2(\underline{\underline{s}}^*) + A(H+3\mu)F(\underline{\underline{s}} - \underline{\underline{a}}_1)F(\underline{\underline{s}}^*) - B(H+3\mu)PF(\underline{\underline{s}} - \underline{\underline{a}}_1) \tag{47}$$

$$X = \frac{1}{2L}\left(-M + \sqrt{M^2 - 4LN}\right) \tag{48}$$

However, even with this choice of signs in front of the radical, the sign of the solution is not clear because it depends on that of N, which is not itself clear (even with B small.) It is therefore not impossible that Eq. (48) provides a negative root. In this case, it is better to adopt another algorithm which may be less precise but certainly leads to a positive root. It suffices for this purpose to replace the expressions Eq. (23) and Eq. (24), semi-implicit with respect to the norm of $\underline{\underline{s}} - \underline{\underline{a}}_1$, by the implicit expressions:

$$(\Delta \underline{\underline{\varepsilon}}^p)' = A(\underline{\underline{s}} + \Delta \underline{\underline{s}} - \underline{\underline{a}}_1 - \Delta \underline{\underline{a}}_1) \tag{23'}$$

$$(\Delta \underline{\underline{\varepsilon}}^p)'' = B(\Delta \sigma_1^{eq})_s(\underline{\underline{s}} + \Delta \underline{\underline{s}} - \underline{\underline{a}}_1 - \Delta \underline{\underline{a}}_1) \tag{24'}$$

$$L'X^2 + M'X + N' = 0 \tag{44'}$$

We can see that to find these epressions from Eq. (23) and Eq. (24), we shall replace $F(\underline{\underline{s}} - \underline{\underline{a}}_1)$ by $F\left(\underline{\underline{s}} + \Delta \underline{\underline{s}} - \underline{\underline{a}}_1 - \Delta \underline{\underline{a}}_1\right) \equiv X$. We obtain therefore the same equation Eq. (44) on X as previously, but by performing this substitution in the expressions Eq. (45), Eq. (46) and Eq. (47) of L, M, N, this equation becomes

$$L' = 6\mu B F(\underline{\underline{s}}^*) \tag{45'}$$

$$M' = 2BHF^2(\underline{\underline{s}}^*) + 2A(H + 3\mu)F(\underline{\underline{s}}^*) - 2B(H + 3\mu)P \tag{46'}$$

$$N = -3F^2(\underline{\underline{s}}^*) \tag{47'}$$

The coefficients L' and N' are here clearly positive and negative, respectively; therefore the product of the roots N'/L' is negative, so that there are two roots reals, one positive and the other one negative, as desired; the positive root is

$$X = \frac{1}{2L'}\left(-M' + \sqrt{M'^2 - 4L'N'}\right) \tag{48'}$$

Once X is calculated by Eq. (48), we can deduce Y by equation Eq. (42) (eventually by replacing $F(\underline{\underline{s}} - \underline{\underline{a}}_1)$ by X), $\underline{\underline{s}} + \Delta \underline{\underline{s}} - \underline{\underline{a}}_1 - \Delta \underline{\underline{a}}_1$ by Eq. (41), $(\Delta \underline{\underline{\varepsilon}}^p)' + (\Delta \underline{\underline{\varepsilon}}^p)''$ by Eq. (39) (by replacing again eventually X by $F(\underline{\underline{s}} - \underline{\underline{a}}_1)$), $\underline{\underline{s}} + \Delta \underline{\underline{s}}$ by Eq. (35). It remains to update the parameter of strain hardening. The variations of ε_2^{eff} and $\underline{\underline{a}}_2$ are given by Eq. (30) and Eq. (32). The variations of ε_2^{eff} and and $\underline{\underline{a}}_2$ are obtained from Eq. (31) and Eq. (33) which can be re-written as

$$\varepsilon_2^{eff}\Delta z + (z + \Delta z)\varepsilon_2^{eff} = \theta \varepsilon_1^{eff}\Delta z \Rightarrow \Delta \varepsilon_2^{eff} = \frac{\Delta z}{z + \Delta z}(-\varepsilon_2^{eff} + \theta \varepsilon_1^{eff}) \tag{49}$$

$$\begin{aligned} &\underline{\underline{a}}_2 \Delta z + (z + \Delta z)\Delta \underline{\underline{a}}_2 = \theta \underline{\underline{a}}_1 \Delta z - z(\Delta \underline{\underline{a}}_2)_{GT} + z(\Delta \underline{\underline{a}}_2)_T \Rightarrow \\ &\Delta \underline{\underline{a}}_2 = \frac{1}{z + \Delta z}\left[(-\underline{\underline{a}}_2 + \theta \underline{\underline{a}}_1)\Delta z - z(\Delta \underline{\underline{a}}_2)_{GT} + z(\Delta \underline{\underline{a}}_2)_T\right] \end{aligned} \tag{50}$$

(Let us note that due the discretization explicit of $\Delta\underline{\underline{a}}_2)_{GT}$ and $(\Delta\underline{\underline{a}}_2)_T$, the variations of ε_2^{eff} and $\underline{\underline{a}}_2$ can, in fact, be calculated at the beginning, before the calculation of X and Y.)

$$\sigma_{eq} + \Delta\sigma_{eq} \equiv F(\underline{\underline{s}} + \Delta\underline{\underline{s}} - \underline{\underline{a}} - \Delta\underline{\underline{a}}) < \sigma^Y + \Delta\sigma^Y \tag{51}$$

It is finally necessary to verify the stress-limit condition not reached. defining the case considered. The calculation of $\sigma^Y + \Delta\sigma^Y$ is immediate knowing $\varepsilon_1^{eff} + \Delta\varepsilon_1^{eff}$, $\varepsilon_2^{eff} + \Delta\varepsilon_2^{eff}$, $z + \Delta z$, $T + \Delta T$. Finding the value of $\sigma_{eq} + \Delta\sigma_{eq}$ necessitates to evaluate $(\underline{\underline{s}} + \Delta\underline{\underline{s}} - \underline{\underline{a}} - \Delta\underline{\underline{a}}$. We obtain:

$$\underline{\underline{s}} + \Delta\underline{\underline{s}} - \underline{\underline{a}} - \Delta\underline{\underline{a}} = \underline{\underline{s}} + \Delta\underline{\underline{s}} - (1 - z - \Delta z)(\underline{\underline{a}}_1 + \Delta\underline{\underline{a}}_1) - (z + \Delta z)(\underline{\underline{a}}_2 + \Delta\underline{\underline{a}}_2)$$

All tensors being known here, we deduce $(\underline{\underline{s}} + \Delta\underline{\underline{s}} - \underline{\underline{a}} - \Delta\underline{\underline{a}}$. However, we can calculate this expression before evaluating $\Delta\underline{\underline{a}}_1$ using X, Y and the tensors known a priori $\underline{\underline{s}}^\star$, $\left(\Delta\underline{\underline{a}}_1\right)_{GT}$, $\left(\Delta\underline{\underline{a}}_1\right)_T$ and $\Delta\underline{\underline{a}}_2$. Indeed, from Eq.(32) and Eq.(39),

$$\underline{\underline{a}}_1 + \Delta\underline{\underline{a}}_1 = \underline{\underline{a}}_1 + \frac{H}{3}(A + BY)\left(1 + \frac{F(\underline{\underline{s}} - \underline{\underline{a}}_1)}{X}\right)(\underline{\underline{s}} + \Delta\underline{\underline{s}} - \underline{\underline{a}}_1 - \Delta\underline{\underline{a}}_1) \\ -(\Delta\underline{\underline{a}}_1)_{GT} + (\Delta\underline{\underline{a}}_1)_T$$

where we deduce, using the previous expression of $(\underline{\underline{s}} + \Delta\underline{\underline{s}} - \underline{\underline{a}} - \Delta\underline{\underline{a}}$ and Eq.(41):

$$\begin{aligned}
\underline{\underline{s}} + \Delta\underline{\underline{s}} - \underline{\underline{a}} - \Delta\underline{\underline{a}} &= \underline{\underline{s}} + \Delta\underline{\underline{s}} - \underline{\underline{a}}_1 - \Delta\underline{\underline{a}}_1 + (z + \Delta z)(\underline{\underline{a}}_1 + \Delta\underline{\underline{a}}_1 - \underline{\underline{a}}_2 - \Delta\underline{\underline{a}}_2) \\
&= \left[1 + (z + \Delta z)\frac{H}{3}(A + BY)\left(1 + \frac{F(\underline{\underline{s}} - \underline{\underline{a}}_1)}{X}\right)\right](\underline{\underline{s}} + \Delta\underline{\underline{s}} - \underline{\underline{a}}_1 - \Delta\underline{\underline{a}}_1) \\
&+ (z + \Delta z)(\underline{\underline{a}}_1 - (\Delta\underline{\underline{a}}_1)_{GT} + (\Delta\underline{\underline{a}}_1)_T - \underline{\underline{a}}_2 - \Delta\underline{\underline{a}}_2) \\
&= \left[X + (z + \Delta z)\frac{H}{3}(A + BY)\left(X + F(\underline{\underline{s}} - \underline{\underline{a}}_1)\right)\right]\frac{\underline{\underline{s}}^*}{F(\underline{\underline{s}}^*)} \\
&+ (z + \Delta z)(\underline{\underline{a}}_1 - (\Delta\underline{\underline{a}}_1)_{GT} + (\Delta\underline{\underline{a}}_1)_T - \underline{\underline{a}}_2 - \Delta\underline{\underline{a}}_2)
\end{aligned} \tag{52}$$

(of course, it is still possible to substitute X with $F(\underline{\underline{s}} - \underline{\underline{a}})$ in this expression).

5.2. Case where the limit stress is reached

The discretized equations can be written as:

$$\Delta\underline{\underline{e}} = \Delta\underline{\underline{e}}^e + \Delta\underline{\underline{\varepsilon}}^P \tag{53}$$

$$\sigma_{eq} + \Delta\sigma_{eq} \equiv F(\underline{\underline{s}} + \Delta\underline{\underline{s}} - \underline{\underline{a}} - \Delta\underline{\underline{a}}) = \sigma^Y(\varepsilon_1^{eff} + \Delta\varepsilon_1^{eff}, \varepsilon_2^{eff} + \Delta\varepsilon_2^{eff}, z + \Delta z, T + \Delta T) \tag{54}$$

$$\Delta\underline{\underline{\sigma}}^P = \frac{3}{2}\frac{\Delta\varepsilon_{eq}}{F(\underline{\underline{s}} + \Delta\underline{\underline{s}} - \underline{\underline{a}} - \Delta\underline{\underline{a}})}(\underline{\underline{s}} + \Delta\underline{\underline{s}} - \underline{\underline{a}} - \Delta\underline{\underline{a}}) \tag{55}$$

$$\begin{aligned} &\Delta\underline{\underline{s}}_{OBJ} = \Delta\underline{\underline{s}} + (\Delta\underline{\underline{s}})_{GT} = 2\mu\Delta\underline{\underline{e}}^e + (\Delta\underline{\underline{s}})_T \\ &\Rightarrow \Delta\underline{\underline{s}} = 2\mu\Delta\underline{\underline{e}}^e - (\Delta\underline{\underline{s}})_{GT} + (\Delta\underline{\underline{s}})_T \end{aligned} \tag{56}$$

$$\Delta\varepsilon_1^{eff} = \Delta\varepsilon_{eq} \tag{57}$$

$$\begin{aligned} &\Delta(z\varepsilon_2^{eff}) = \left(z + \frac{\Delta z}{2}\right)\Delta\varepsilon_{eq} + \theta\varepsilon_1^{eff}\Delta z \Rightarrow \\ &\Delta\varepsilon_2^{eff} = \frac{1}{z + \Delta z}\left[\left(z + \frac{\Delta z}{2}\right)\Delta\varepsilon_{eq} + (-\varepsilon_2^{eff} + \theta\varepsilon_1^{eff})\Delta z\right] \end{aligned} \tag{58}$$

$$\begin{aligned} &(\Delta\underline{\underline{a}}_1)_{OBJ} = \Delta\underline{\underline{a}}_1 + (\Delta\underline{\underline{a}}_1)_{GT} = \frac{2}{3}(1-p)\frac{\Delta\overline{\sigma}_1}{\Delta\varepsilon_1^{eff}}\Delta\varepsilon^p + (\Delta\underline{\underline{a}}_1)_T \Rightarrow \\ &\Delta\underline{\underline{a}}_1 = \frac{2}{3}(1-p)\frac{\Delta\overline{\sigma}_1}{\Delta\varepsilon_1^{eff}}\Delta\varepsilon^p - (\Delta\underline{\underline{a}}_1)_{GT} + (\Delta\underline{\underline{a}}_1)_T \end{aligned} \tag{59}$$

$$\Delta(z\underline{\underline{a}}_2) = \frac{2}{3}(1-p)(z + \frac{\Delta z}{2})\frac{\Delta\overline{\sigma}_2}{\Delta\varepsilon_2^{eff}}\Delta\varepsilon^p + \theta\underline{\underline{a}}_1\Delta z - z(\Delta\underline{\underline{a}}_2)_{GT} + z(\Delta\underline{\underline{a}}_2)_T \tag{60}$$

The quantities $\Delta\overline{\sigma}_1/\Delta\varepsilon_1^{eff}$ and $\Delta\overline{\sigma}_2/\Delta\varepsilon_2^{eff}$ intervening in the evolutions equations of the parameters of the kinematic hardening are here the secant of strain hardening defined by

$$\frac{\Delta\overline{\sigma}_i}{\Delta\varepsilon_i^{eff}} = \frac{1}{\Delta\varepsilon_i^{eff}}\left[\overline{\sigma}_i(\varepsilon_i^{eff} + \Delta\varepsilon_i^{eff}, T + \Delta T) - \overline{\sigma}_i(\varepsilon_i^{eff}, T + \Delta T)\right] \tag{61}$$

This choice rather than that of the slopes of work hardening, as previously, is justified by compatibility with the resolution which follows, which will naturally make use again of the secants, this time for the isotropic part of the work hardening, via

the exact respect of the criterion at the time $t+\Delta t$. Note also that Eq.(60) will be used in the given form, and not in the form of an expression of $\Delta\underline{\underline{a}}_2$ which will be less convenient here.

Now let us solve these equations by adopting $\Delta\varepsilon_{eq}$ as a key unknown. Proceeding as before from Eq.(53) and Eq.(56), we obtain

$$\underline{\underline{s}}+\Delta\underline{\underline{s}}=\underline{\underline{s}}+2\mu\Delta\underline{\underline{e}}-(\Delta\underline{\underline{s}})_{GT}+(\Delta\underline{\underline{s}})_T-2\mu\Delta\varepsilon^p$$

which, by assuming as previously

$$(\underline{\underline{s}}+\Delta\underline{\underline{s}})^{el}=\underline{\underline{s}}+2\mu\Delta\underline{\underline{e}}-(\Delta\underline{\underline{s}})_{GT}+(\Delta\underline{\underline{s}})_T \tag{62}$$

and using Eq.(55), is equivalent to

$$\underline{\underline{s}}+\Delta\underline{\underline{s}}=(\underline{\underline{s}}+\Delta\underline{\underline{s}})^{el}-3\mu\frac{\Delta\varepsilon_{eq}}{F(\underline{\underline{s}}+\Delta\underline{\underline{s}}-\underline{\underline{a}}-\Delta\underline{\underline{a}})}(\underline{\underline{s}}+\Delta\underline{\underline{s}}-\underline{\underline{a}}-\Delta\underline{\underline{a}})$$

By adding $-\underline{\underline{a}}-\Delta\underline{\underline{a}}$ to the two sides of the equations, and by writing $\underline{\underline{a}}+\Delta\underline{\underline{a}}$ in the form

$$\underline{\underline{a}}+\Delta\underline{\underline{a}}=(1-z-\Delta z)(\underline{\underline{a}}_1+\Delta\underline{\underline{a}}_1)+z\underline{\underline{a}}_2+\Delta(z\underline{\underline{a}}_2)$$

and using Eq.(59) and Eq.(60), we get

$$\begin{aligned}\underline{\underline{s}}+\Delta\underline{\underline{s}}-\underline{\underline{a}}-\Delta\underline{\underline{a}}=&(\underline{\underline{s}}+\Delta\underline{\underline{s}})^{el}-3\mu\frac{\Delta\varepsilon_{eq}}{F(\underline{\underline{s}}+\Delta\underline{\underline{s}}-\underline{\underline{a}}-\Delta\underline{\underline{a}})}(\underline{\underline{s}}+\Delta\underline{\underline{s}}-\underline{\underline{a}}-\Delta\underline{\underline{a}})\\&-(1-z-\Delta z)(\underline{\underline{a}}_1+\Delta\underline{\underline{a}}_1)-z\underline{\underline{a}}_2-\Delta(z\underline{\underline{a}}_2)\\&=(\underline{\underline{s}}+\Delta\underline{\underline{s}})^{el}-(1-z-\Delta z)\left[\underline{\underline{a}}_1-(\Delta\underline{\underline{a}}_1)_{GT}+(\Delta\underline{\underline{a}}_1)_T\right]-z\underline{\underline{a}}_2\\&-3\mu\frac{\Delta\varepsilon_{eq}}{F(\underline{\underline{s}}+\Delta\underline{\underline{s}}-\underline{\underline{a}}-\Delta\underline{\underline{a}})}(\underline{\underline{s}}+\Delta\underline{\underline{s}}-\underline{\underline{a}}-\Delta\underline{\underline{a}})\\&-(1-z-\Delta z)\frac{2}{3}(1-p)\frac{\Delta\overline{\sigma}_1}{\Delta\varepsilon_1^{\mathit{eff}}}\cdot\frac{3}{2}\frac{\Delta\varepsilon_{eq}}{F(\underline{\underline{s}}+\Delta\underline{\underline{s}}-\underline{\underline{a}}-\Delta\underline{\underline{a}})}(\underline{\underline{s}}+\Delta\underline{\underline{s}}-\underline{\underline{a}}-\Delta\underline{\underline{a}})\\&-\frac{2}{3}(1-p)(z+\frac{\Delta z}{2})\frac{\Delta\overline{\sigma}_2}{\Delta\varepsilon_2^{\mathit{eff}}}\cdot\frac{3}{2}\frac{\Delta\varepsilon_{eq}}{F(\underline{\underline{s}}+\Delta\underline{\underline{s}}-\underline{\underline{a}}-\Delta\underline{\underline{a}})}(\underline{\underline{s}}+\Delta\underline{\underline{s}}-\underline{\underline{a}}-\Delta\underline{\underline{a}})\\&-\theta\underline{\underline{a}}_1\Delta z+z(\Delta\underline{\underline{a}}_2)_{GT}-z(\Delta\underline{\underline{a}}_2)_T\end{aligned}$$

By using

$$\begin{aligned}\underline{\underline{s}}^*\quad&\equiv(\underline{\underline{s}}+\Delta\underline{\underline{s}})^{el}-(1-z-\Delta z)\left[\underline{\underline{a}}_1-(\Delta\underline{\underline{a}}_1)_{GT}+(\Delta\underline{\underline{a}}_1)_T\right]\\&\quad-z\underline{\underline{a}}_2-\theta\underline{\underline{a}}_1\Delta z+z(\Delta\underline{\underline{a}}_2)_{GT}-z(\Delta\underline{\underline{a}}_2)_T\end{aligned} \tag{63}$$

(note that this definition is not the same as that of Eq.(37), in the case where the stress limit is not reached), and

$$\widetilde{H}\equiv(1-z-\Delta z)(1-p)\frac{\Delta\overline{\sigma}_1}{\Delta\varepsilon_1^{\mathit{eff}}}+(z+\frac{\Delta z}{2})(1-p)\frac{\Delta\overline{\sigma}_2}{\Delta\varepsilon_2^{\mathit{eff}}} \tag{64}$$

this can be written as

$$\left[1+\frac{\left(\widetilde{H}+3\mu\right)\Delta\varepsilon_{eq}}{F(\underline{\underline{s}}+\Delta\underline{\underline{s}}-\underline{\underline{a}}-\Delta\underline{\underline{a}})}\right](\underline{\underline{s}}+\Delta\underline{\underline{s}}-\underline{\underline{a}}-\Delta\underline{\underline{a}})=\underline{\underline{s}}^{*} \tag{65}$$

Before going any further, let us give a simple and more meaningful expression of $\underline{\underline{s}}^{*}$. Let us denote $\underline{\underline{a}}_1+(\Delta\underline{\underline{a}}_1)_{GT,T}$ and $\underline{\underline{a}}_2+(\Delta\underline{\underline{a}}_2)_{GT,z,T}$ the values of $\underline{\underline{a}}_1$ and $\underline{\underline{a}}_2$ obtained by taking into account, in the variation $\Delta\underline{\underline{a}}_1$ and $\Delta\underline{\underline{a}}_2$, only the terms due to large transformations and variations of z and T (that is omitting the term proportional to $\Delta\underline{\underline{\varepsilon}}^{p}$). We have, by Eq.(59) and Eq.(60):

$$\underline{\underline{a}}_1+(\Delta\underline{\underline{a}}_1)_{GT,T}=\underline{\underline{a}}_1-(\Delta\underline{\underline{a}}_1)_{GT}+(\Delta\underline{\underline{a}}_1)_{T},$$

$$\begin{aligned}&(z+\Delta z)\lfloor\underline{\underline{a}}_2+(\Delta\underline{\underline{a}}_2)_{GT,z,T}\rfloor-z\underline{\underline{a}}_2=\theta\underline{\underline{a}}_1\Delta z-z(\Delta\underline{\underline{a}}_2)_{GT}+z(\Delta\underline{\underline{a}}_2)_{T}\\&\Rightarrow(z+\Delta z)\lfloor\underline{\underline{a}}_2+(\Delta\underline{\underline{a}}_2)_{GT,z,T}\rfloor=z\underline{\underline{a}}_2+\theta\underline{\underline{a}}_1\Delta z-z(\Delta\underline{\underline{a}}_2)_{GT}+z(\Delta\underline{\underline{a}}_2)_{T}\end{aligned}$$

From these two expressions and Eq.(63) we can deduce that

$$\begin{aligned}\underline{\underline{s}}^{*}=(\underline{\underline{s}}+\Delta\underline{\underline{s}})^{el}-(1-z-\Delta z)\lfloor\underline{\underline{a}}_1+(\Delta\underline{\underline{a}}_1)_{GT,z,T}\rfloor-\\(z+\Delta z)\lfloor\underline{\underline{a}}_2+(\Delta\underline{\underline{a}}_2)_{GT,z,T}\rfloor\end{aligned} \tag{66}$$

This expression allows an easy calculation of $\underline{\underline{s}}^{*}$, having previously carried out the pre-corrections of $\underline{\underline{a}}_1$ and $\underline{\underline{a}}_2$ due to large transformations and variations of z and T. Eq.(65) implies that the (unknown) tensor $\underline{\underline{s}}+\Delta\underline{\underline{s}}-\underline{\underline{a}}-\Delta\underline{\underline{a}}$ is positively collinear with the (known) tensor, $\underline{\underline{s}}^{*}$; thereby

$$\underline{\underline{s}}+\Delta\underline{\underline{s}}-\underline{\underline{a}}-\Delta\underline{\underline{a}}=\frac{F(\underline{\underline{s}}+\Delta\underline{\underline{s}}-\underline{\underline{a}}-\Delta\underline{\underline{a}})}{F(\underline{\underline{s}}^{*})}\underline{\underline{s}}^{*} \tag{67}$$

In addition, we obtain by taking the Von Mises function of the two sides of Eq.(65):

$$F(\underline{\underline{s}}+\Delta\underline{\underline{s}}-\underline{\underline{a}}-\Delta\underline{\underline{a}})+(\widetilde{H}+3\mu)\Delta\varepsilon_{eq}=F(\underline{\underline{s}}^{*}) \tag{68}$$

The equation Eq.(54) gives, by expliciting the yield limit thanks Eq.(6):

$$\begin{aligned}F(\underline{\underline{s}}+\Delta\underline{\underline{s}}-\underline{\underline{a}}-\Delta\underline{\underline{a}})&=[1-f(z+\Delta z)]\,\sigma_1^{Y}(\varepsilon_1^{\mathit{eff}}+\Delta\varepsilon_1^{\mathit{eff}},T+\Delta T)\\&+f(z+\Delta z)\sigma_2^{Y}(\varepsilon_2^{\mathit{eff}}+\Delta\varepsilon_2^{\mathit{eff}},T+\Delta T)\\&=[1-f(z+\Delta z)]\left[\sigma_1^{Y}(\varepsilon_1^{\mathit{eff}},T+\Delta T)+p\frac{\Delta\overline{\sigma}_1}{\Delta\varepsilon_1^{\mathit{eff}}}\Delta\varepsilon_1^{\mathit{eff}}\right]\\&+f(z+\Delta z)\left[\sigma_2^{Y}(\varepsilon_1^{\mathit{eff}},T+\Delta T)+p\frac{\Delta\overline{\sigma}_2}{\Delta\varepsilon_2^{\mathit{eff}}}\Delta\varepsilon_2^{\mathit{eff}}\right]\\&=\sigma^{Y}(\varepsilon_1^{\mathit{eff}},\varepsilon_2^{\mathit{eff}},z+\Delta z,T+\Delta T)\\&+[1-f(z+\Delta z)]\,p\frac{\Delta\overline{\sigma}_1}{\Delta\varepsilon_1^{\mathit{eff}}}\Delta\varepsilon_1^{\mathit{eff}}+f(z+\Delta z)p\frac{\Delta\overline{\sigma}_2}{\Delta\varepsilon_2^{\mathit{eff}}}\Delta\varepsilon_2^{\mathit{eff}}\end{aligned}$$

which gives, by reporting in Eq.(68):

$$\sigma^Y(\varepsilon_1^{eff}, \varepsilon_2^{eff}, z+\Delta z, T+\Delta T) + [1-f(z+\Delta z)]\, p\frac{\Delta\overline{\sigma}_1}{\Delta\varepsilon_1^{eff}}\Delta\varepsilon_1^{eff}$$
$$+ f(z+\Delta z)p\frac{\Delta\overline{\sigma}_2}{\Delta\varepsilon_2^{eff}}\Delta\varepsilon_2^{eff} + (\widetilde{H}+3\mu)\Delta\varepsilon_{eq} = F(\underline{\underline{s}}^*)$$

This equation can be written as, according to Eq.(57) and Eq.(58):

$$(H+3\mu)\Delta\varepsilon_{eq} = \Delta \tag{69}$$

$$\begin{aligned} H \quad &\equiv \widetilde{H} + [1-f(z+\Delta z)]\, p\frac{\Delta\overline{\sigma}_1}{\Delta\varepsilon_1^{eff}} + f(z+\Delta z)\frac{z+\Delta z/2}{z+\Delta z}p\frac{\Delta\overline{\sigma}_2}{\Delta\varepsilon_2^{eff}} \\ &= (1-z-\Delta z)(1-p)\frac{\Delta\overline{\sigma}_1}{\Delta\varepsilon_1^{eff}} + \left(z+\frac{\Delta z}{2}\right)(1-p)\frac{\Delta\overline{\sigma}_2}{\Delta\varepsilon_2^{eff}} \\ &+ [1-f(z+\Delta z)]\, p\frac{\Delta\overline{\sigma}_1}{\Delta\varepsilon_1^{eff}} + f(z+\Delta z)\frac{z+\Delta z/2}{z+\Delta z}p\frac{\Delta\overline{\sigma}_2}{\Delta\varepsilon_2^{eff}} \end{aligned} \tag{70}$$

$$\Delta \equiv F(\underline{\underline{s}}^*) - \sigma_1^Y(\varepsilon_1^{eff} + \Delta\varepsilon_1^{eff}, T+\Delta T) + f(z+\Delta z)p\frac{\Delta\overline{\sigma}_2}{\Delta\varepsilon_2^{eff}}\frac{\Delta z}{z+\Delta z}\times$$
$$(\varepsilon_2^{eff} - \theta\varepsilon_1^{eff}) \tag{71}$$

Eq.(69) relates to the only unknown $\Delta\varepsilon_{eq}$, the strain hardening secants depends on the ε_1^{eff} which are expressed as a function of $\Delta\varepsilon_{eq}$, thanks to the equations Eq.(57) and Eq.(58). It can be solved, for example, by the method of the fixed point. The quantity $F(\underline{\underline{s}} + \Delta\underline{\underline{s}} - \underline{\underline{a}} - \Delta\underline{\underline{a}})$ is then deduced from Eq.(54), and then the tensor $\underline{\underline{s}} + \Delta\underline{\underline{s}} - \underline{\underline{a}} - \Delta\underline{\underline{a}}$ is deduced from Eq.(67). Finalyy, we calculate $\Delta\underline{\underline{\varepsilon}}^p$ thanks to Eq.(55), then $\underline{\underline{a}}_1$ and $\underline{\underline{a}}_2$ thanks to Eq.(59) and Eq.(60).

5.3. Particular case: isotropic strain hardening with the yield limit not reached

If the yield limit is not reached, the expression of Eq.(27) proposed for $(\Delta\sigma_1^{eq})_s$ is applicable whatever the type of the work hardening. However, for a pure isotropic work hardening $p \equiv 1$ is equivalent to the expression Eq.(10) of $(\dot{\sigma}_1^{eq})_s$ can also be written equivalently (with ($\underline{\underline{a}}_1 \equiv \underline{\underline{0}}$)) as:

$$(\dot{\sigma}_1^{eq})_s \equiv \frac{3}{2\sigma^{eq}} \underline{\underline{s}} : \overset{\circ}{\underline{\underline{s}}} = \dot{\sigma_{eq}} \quad , \quad \sigma_{eq} \equiv \left(\frac{3}{2} \underline{\underline{s}} : \underline{\underline{s}} \right)^{\frac{1}{2}}$$

We can then assume that a simple expression for $(\Delta\sigma_1^{eq})_s$, than Eq.(27)

$$(\Delta\sigma_1^{eq})_s \equiv Y \equiv \Delta\sigma_{eq} = F(\underline{\underline{s}} + \Delta\underline{\underline{s}}) - F(s) \equiv X - F(\underline{\underline{s}}) \qquad (27'')$$

This simplification is adopted in several finite element codes. It is necessary to take again the elements of the numerisation exposed in the Section 4.1 in the case of the purely isotropic work hardening where the yield stress is not reached.

The equation Eq.(40) being obtained without using the expression Eq.(27) of $(\Delta\sigma_1^{eq})_s \equiv Y \equiv \Delta\sigma_{eq}$ is valid here also; it can be written as, with $\underline{\underline{a}}_1 \equiv \underline{\underline{0}}$, $\Delta\underline{\underline{a}}_1 \equiv \underline{\underline{0}}$, $p \equiv 1$ (thus, $H = 0$ from Eq.(38)):

$$\left[1 + \mu(A + BY) \left(1 + \frac{F(\underline{\underline{s}})}{X} \right) \right] (\underline{\underline{s}} + \Delta\underline{\underline{s}}) = \underline{\underline{s}}^*$$

$\underline{\underline{s}}^*$ is always given by Eq.(37), with $\underline{\underline{a}}_1 \equiv \underline{\underline{0}}$, $(\Delta\underline{\underline{a}}_1)_T \equiv \underline{\underline{0}}$

$$X + \mu(A + BY)(X + F(\underline{\underline{s}})) = X + \mu[A + B(X - F(\underline{\underline{s}}))](X + F(\underline{\underline{s}})) = F(\underline{\underline{s}}^*)$$

The equation Eq.(41) then applied always, with $\underline{\underline{a}}_1 \equiv \underline{\underline{0}}$, $\Delta\underline{\underline{a}}_1 \equiv \underline{\underline{0}}$. In addition, taking into account the function of Von Mises of the two sides of Eq.(40") and taking into account Eq.(27"), we obtain:

$$L''X^2 + M''X + N'' = 0 \qquad (44'')$$

which gives by re-ordering the terms

$$L'' + \mu B \qquad (45'')$$

$$M'' = 1 + \mu A \qquad (46'')$$

$$N'' = \mu A F(\underline{\underline{s}}) - \mu B F^2(\underline{\underline{s}}) - F(\underline{\underline{s}}^*) \qquad (47'')$$

As in the usual case, this formulation does not necessarily ensure that there exists a positive real solution X. If this is not the case, we can adopt a completely implicit algorithm (replacement of Eq.(23) and Eq.(24) by Eq.(23') and Eq.(24'). This leads to replacing $F(\underline{\underline{s}})$ by $F(\underline{\underline{s}} + \Delta\underline{\underline{s}} \equiv X$ in Eq.(40'), which becomes:

$$[1 + 2\mu(A + BY)](\underline{\underline{s}} + \Delta\underline{\underline{s}}) = \underline{\underline{s}}^* \qquad (40'')$$

By taking the von Mises function of the two sides of the previous equations and taking into account Eq.(27''), we then obtain

$$X + 2\mu X[A + B(X - F(\underline{\underline{s}}))] = F(\underline{\underline{s}}^*)$$

which is equivalent to

$$L'''X^2 + M'''X + N''' = 0 \qquad (44'')$$

$$L''' + 2\mu B \qquad (45'')$$

$$M''' = 1 + 2\mu(A - BF(\underline{\underline{s}})) \qquad (46'')$$

$$N''' = -F(\underline{\underline{s}}^*) \qquad (47'')$$

Since $L''' > 0$ and $N''' > 0$, the existence of this unique psoitve solution is therefore guaranteed.

6. Numerical Results / Comparisons with Experiments / Discussion

The algorithm described above is implemented in SYSTUS to evaluate the model described above. The numerical modeling pertains to a martensitic transformation of A508 steel. The transformation deformation is solely induced by thermal deformation (the expansion of the daughter phase) without including any deviatoric component (neglecting shape change). The results of this modeling provide a better understanding of the behavior of A508 steel during its martensitic transformation. This data is crucial for optimizing heat treatment processes and designing A508 steel components for specific applications, such as nuclear construction. The thermo-mechanical properties assumed for the two phases are as follows:

The transformation of an element occurs through a change in its thermo-elastic properties from phase γ to phase α. During this transformation, a uni-axial stress with a constant amplitude of approximately $1/3$ of the yield strength of the weaker phase is applied to the material. This study demonstrates that the first type of transformation (diffusive progression of the elements to be transformed) provides a better agreement with the theoretical predictions of the author's analytical model.

We will numerically investigate transformation plasticity, focusing on Greenwood and Johnson's mechanism. In this study, a finite element mesh will undergo external loading, with sequential element transformations other by changing their thermal strain and yield stress from those of the γ phase to those of the α phase. The transformation strain will consist only of the difference of thermal strain between the phases and will not include any deviatoric part (change of shape). The transformation studied is the martensitic transformation of the A.508 cl. 3 steel. The temperature dependence of the thermo-mechanical characteristics is disregarded. These characteristics are provided in the document Appendix A appended to this paper.

The chosen Representative Elementary Volume (REV) for modeling transformation plasticity is a regular $5 \times 5 \times 5$ mesh cube. The phases exhibit perfectly plastic behavior (without hardening). Two types of transformations are studied:

1. Elements are transformed in a specific order, from the center of the REV to its boundaries.
2. Elements are transformed in a random order within the REV.

The transformation of an element occurs through a change in its thermo-elastic properties from phase γ to phase α. During this transformation, a uni-axial stress with a constant amplitude of about $1/3$ of the yield strength of the weakest phase is applied to the REV.

This study demonstrates that the first type of transformation (diffusive progression of the elements to be transformed) provides a better agreement with the theoretical predictions of the author's analytical model.

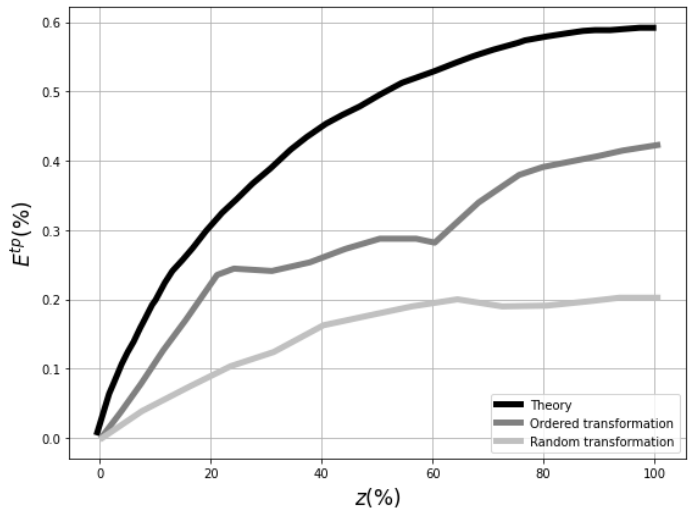

Figure 1: Transformation plastic strain in a 5 $\times$ 5 $\times$ 5 cube for a stress equals to 50 MPa : 1) Theory; 2) Ordered transformation, $\Sigma_{xx} = 50$ MPa; 3) Random transformation

Figure 1 illustrates the plastic strain resulting from transformation in a 5 $\times$ 5 $\times$ 5 cube under an applied stress of 50 MPa, capturing both ordered and random transformations. This visual depiction serves as a comprehensive snapshot of the material's response to the specified stress conditions, offering a comparative analysis between the two transformation scenarios.

Examining the intricate dynamics of the random transformation process reveals a captivating interplay between theoretical expectations and empirical observations. The conspicuous deviation in the associated curve from the theoretical baseline serves as an intriguing cue, inviting us to delve into the nuanced mechanics at play. A critical determinant of this notable discrepancy lies in the profound influence exerted by elements positioned on the surface of the cube.

As the transformation unfolds, the surface elements exhibit a distinctive response characterized by a more facile outward expansion in contrast to their inward progression. This asymmetry in the transformation dynamics stems from the augmented volume experienced by the surface elements during the process. Consequently, the plastic strains induced in the austenitic phase manifest with diminished prominence when compared to their counterparts within the cube's interior. This nuanced phenomenon intricately underpins the underestimation of the Greenwood-Johnson effect, attributing this discrepancy to the ostensibly inconsequential yet influential presence of surface elements.

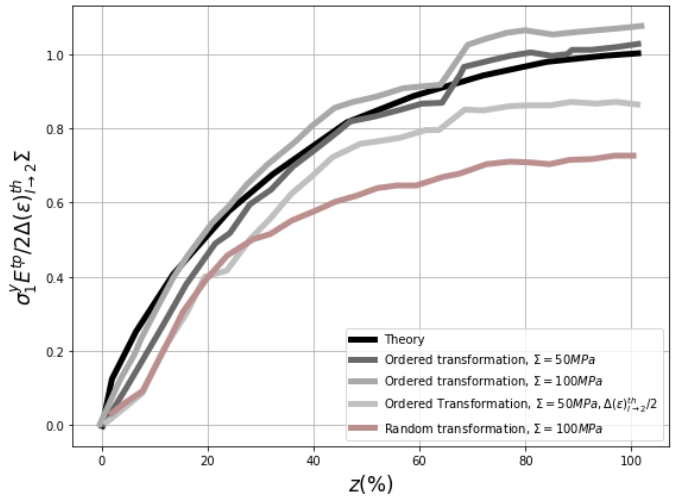

Figure 2: Normalized transformation plastic strain in a 10 $\times$ 10 $\times$ 10 cube for lower stresses : 1) Theory; 2) Ordered transformation, $\Sigma_{xx} = 50$ MPa; 3) Ordered transformation, $\Sigma_{xx} = 100$ MPa; 4) Same as in 2) except that difference of thermal strain between the two phases is divided by 2; 5) random transformation, $\Sigma_{xx} = 100$ MPa

Extending our scrutiny to an ordered transformation originating from the center, a compelling narrative emerges. In the initial stages, wherein only interior elements partake in the transformation, the resultant curve exhibits a slope twice as steep as its random transformation counterpart. This phase aligns seamlessly with theoretical expectations, portraying a harmonious relationship between computation and theory. However, the plot takes a fascinating turn when surface elements become integral to the transformation process.

Upon the involvement of surface elements, a sudden and pronounced decrease in slope unfolds, ushering in a phase marked by a notable misalignment between computational outcomes and theoretical predictions. This inflection point underscores the critical role played by surface elements in shaping the transformation dynamics, offering a deeper understanding of the complex interplay between internal and surface influences on the observed mechanical behavior. In essence, the juxtaposition of random and ordered transformations unravels a rich tapestry of insights, shedding light on the multifaceted nature of material transformations and the consequential impact of seemingly peripheral factors.

Figure 2, serving as the counterpart to Figure 1, replicates the experimental setup, albeit with a diminished mesh size, featuring a cube measuring 10 $\times$ 10 $\times$ 10 units. A notable adjustment in the applied stresses has been introduced, elevating them from 50 MPa to a more substantial 100 MPa. Furthermore, both random and ordered modes of "normalized" transformation were deliberately incorporated into the experimental conditions.

In contrast to its predecessor, Figure 2 encapsulates the same experimental essence but with a finer spatial resolution achieved through a reduced mesh size. The alteration in stress parameters, escalating from 50 MPa to 100 MPa, introduces a heightened mechanical loading scenario, accentuating the influence of external forces on the transformation phenomena. This augmentation in stress levels serves to amplify the mechanical responses within the 10 $\times$ 10 $\times$ 10 cube, providing a nuanced perspective on the material's behavior under varying stress conditions.

The intentional inclusion of both random and ordered transformations in this iteration broadens the scope of the investigation, allowing for a comprehensive analysis of the material's response to distinct transformation mechanisms. This deliberate diversification in transformation types enriches the experimental landscape, facilitating a more thorough exploration of the material's mechanical behavior and its sensitivity to different transformation pathways. The juxtaposition of these transformation modes within the refined experimental setup introduces a layer of complexity, offering a more nuanced understanding of the material's response to varying stress regimes.

It is noteworthy that both transformation orders now yield results that are mutually consistent and align with theoretical expectations. This observation indicates a significant reduction in the influence of surface elements, underscoring the enhanced congruence between the outcomes and theoretical predictions.

We can envisage to investigate the case of very large applied stresses, surpassing the critical yield strength (Σ_y) threshold of 145 MPa. This represents a significant departure from conventional stress levels, introducing a novel challenge in understanding material behavior under extreme conditions.

At such elevated stress levels, it becomes evident that traditional experimental methods and existing theoretical frameworks may no longer suffice to comprehensively capture the intricate nuances of material response. The absence of empirical data and established theories for stress magnitudes beyond $\sigma_y = 145MPa$ underscores the need for alternative approaches to model transformation plasticity.

In this context, numerical simulations emerge as indispensable tools for bridging the knowledge gap. They play a pivotal role in not only compensating for the lack of experimental data but also in establishing a robust and realistic model for transformation plasticity under these unprecedented stress regimes. The reliance on numerical simulations becomes paramount as they offer a flexible and efficient means to explore and comprehend complex material behaviors that elude conventional experimental techniques.

In essence, our exploration of very large applied stresses necessitates a paradigm shift in our approach. The synergy between experimental insights, theoretical frameworks, and numerical simulations is key to advancing our understanding of trans-

formation plasticity under these challenging conditions.

Also, comparisons of the model predictions with experiments conducted on A533 steel transformation plasticity by Desalos [3] serve as a another crucial benchmark for validating our numerical implementation. The insights gained from these comparisons add a significant layer of confidence to the reliability of our simulations. The physical constants employed in our numerical model for this case, characterizing the γ- and α- phases of A533 steel, closely mirror those derived from the meticulous experimental investigations of Desalos [3] and Coret *et al.* [1, 2]. Notably, our material properties feature identical values for Young's modulus ($E = 182,000$ MPa) and Poisson's ratio ($\nu = 0.3$) across both phases, for the rest of the material constants used for the simulations with the A533 steel can be found in Desalos [3] and Coret *et al.* [1, 2].

Furthermore, our choice of yield stress parameters is well-founded, with $\sigma_m = 145\,MPa$ assigned to the mother-phase and $\sigma_D = 950\,MPa$ to the daughter-phase. This meticulous adherence to established values enhances the credibility of our numerical model. Additionally, we account for the relative change of specific volume from the mother- to the daughter-phase. These constants, consistently applied and well-documented, collectively contribute to the robustness of our numerical model, thereby fortifying the reliability and validity of our research findings.

In the examined cases for comparative analysis, the Representative Volume Element (RVE) experiences a uni-axial stress denoted as Σ, consistently applied throughout. This volume undergoes external loading via homogeneous boundary stress (HBStress) or homogeneous boundary strain (HBStrain) conditions to ensure robustness. The primary goal is to strengthen the theoretical analysis, with a specific emphasis on HBStress conditions, while rigorously examining the influence of boundary conditions. The consequential plastic strain transformation along the loading direction is identified as $E_t^p(f)$, capturing the intricate evolution of the material under this specific stress condition. (Any other components are omitted, either being zero or directly correlated to $E_t^p(f)$ owing to considerations of incompressibility.)

In Figure 3, the progression of the transformation plastic strain is depicted, illustrating the dynamic evolution as the transformation unfolds. This evolution is characterized by the ratio $E_t^p(f)/E_t^p(1)$, a metric that ascends from 0 to 1. The dependence on the volume fraction f of the daughter-phase is evident in the plot. The graph not only captures this transformational journey but also highlights the significant variations in the ratio across different values of f.

The depicted data is a comparative analysis involving the predictions of three distinct formulas. Firstly, the original formula (19) proposed by Leblond *et al.*. [8] is represented. Secondly, an allegedly improved variant (20) of the original formula is included in the comparison. Lastly, Desalos [3] introduces a phenomenological formula, $E_t^p(f)/E_t^p(1) \approx f(2-f)$, which he found to be universally applicable to

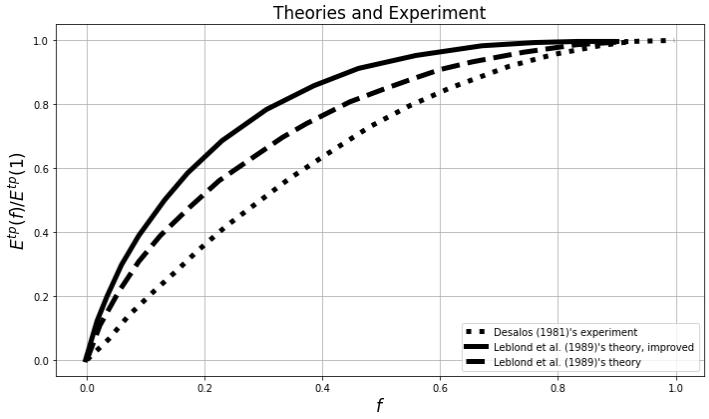

Figure 3: Comparison of evolutions of the transformation plastic strain: Theories and experiments

all his experimental results for the A533 steel, regardless of the stress applied. The juxtaposition of these formulas provides a comprehensive view of their predictive capabilities and sheds light on their performance across the spectrum of volume fractions and stress values.

All theoretical curves, with the exception of the one corresponding to the purportedly enhanced variant of Leblond *et al.*. [8]'s original formula, Eq.11, offer sensible depictions of Desalos [3]'s experimental findings. Nevertheless, across all scenarios, the projected escalation in transformation plastic strain proves somewhat accelerated during the initial half of the transformation process.

In Figure 4, a comparative analysis is presented, juxtaposing the outcomes derived from micro-mechanical simulations conducted under both HBStress and HBStrain conditions. Notably, these simulations were executed under a low stress condition, precisely $\Sigma = 20\,MPa$. It is imperative to highlight that, for contextual reference, the curve representing Desalos [3]'s heuristic formula, previously discussed and applicable across the entire spectrum of stresses he considered, is once again included. This additional visual cue serves as a point of reference, facilitating a comprehensive understanding of the observed results and their alignment with established heuristic models.

A substantial disparity exists in the numerical outcomes derived under HBStress and HBStrain conditions, underscoring the profound impact of boundary conditions. This stark contrast serves to highlight the inherent limitations associated with an approach centered on a simplistic and diminutive Representative Volume Element (RVE), exemplified by a spherical volume of the mother phase housing a solitary growing core of the daughter phase. This discrepancy not only underscores the sensitivity of the results to the chosen boundary conditions but also provides tangible evidence of the inadequacies inherent in employing such a rudimentary RVE model.

Next, we embark on an exploration of the "amplitude" of transformation plasticity, denoted by the value of the transformation plastic strain after the completion of the transformation process, $E_t^p(1)$. In the illustrative Figure 5, this parameter unfolds its dependencies in response to the applied overall stress. Specifically, this juxtaposes diverse perspectives, offering a comprehensive comparison among Leblond *et al.* [8]'s original formula Eq.11, and Desalos[3]'s experimental findings for the A533 steel.

Desalos [3]'s empirical findings, encapsulated in the heuristic formula $E_t^p(1) = 10^{-4}\Sigma$ (with units in MPa), remarkably align with the predicted outcomes, substantiating the robustness and applicability of our general formula Eq.11 in capturing the amplitude of transformation plasticity. This comparative analysis not only serves as a validation of existing models but also unveils the intricate relationship between theoretical predictions and experimental observations in the realm of transformation plasticity, providing a nuanced understanding of material behavior under varying stress conditions.

In Figure 6, a comprehensive comparison unfolds between the predictions derived from our overarching formula Eq.11 and the outcomes gleaned from micromechanical simulations conducted under HBStress and HBStrain conditions. Notably, for reference, Desalos [3]'s experimental results are once again presented, lending an additional layer of context and validation to the juxtaposition of our theoretical predictions with real-world observations.

The numerical outcomes derived under HBStress and HBStrain conditions exhibit a notable disparity, further highlighting the divergence in their respective influences. However, a noteworthy reversal of this trend is observed when considering the ratio $E_t^p(f)/E_t^p(1)$. In contrast to the previous scenario, results associated with HBStrain conditions surpass those under HBStress conditions in this context, with reference to Desalos [3]'s experimental findings.

It becomes apparent that under HBStress conditions, there is a conspicuous tendency for an overestimation of the amplitude of transformation plasticity. This discrepancy underscores the critical role of the chosen stress conditions in influencing the accuracy of predictions, particularly in comparison to experimental benchmarks. The inversion of performance between HBStress and HBStrain conditions underscores the nuanced interplay of factors and the need for a comprehensive understanding of the material response under varying conditions.

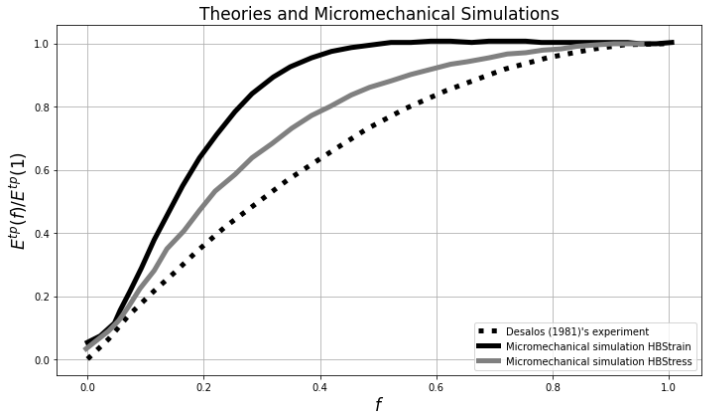

Figure 4: Evolution of Transformation Plastic Strain: A Comparative Analysis between Experiments and Micro-Mechanical Simulations.

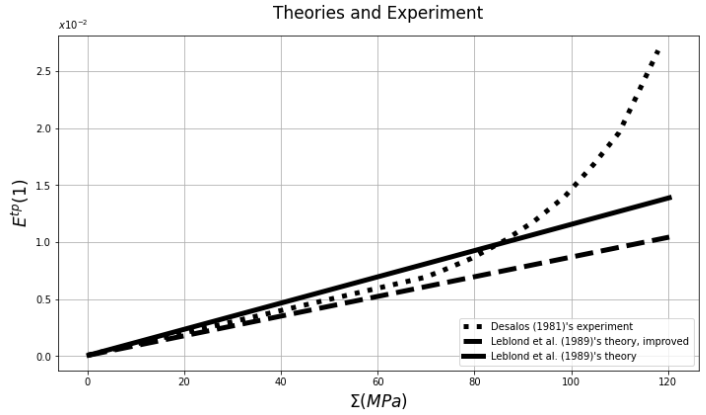

Figure 5: A Comparative Analysis of Plastic Strains Following Full Transformation: Bridging the Divide Between Theoretical Projections and Experimental Realities.

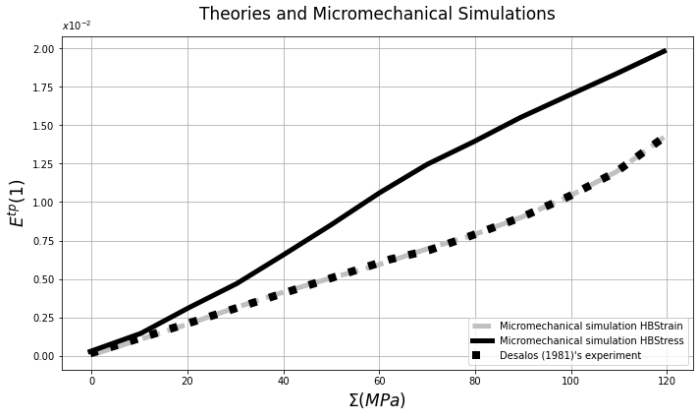

Figure 6: Comparative Analysis of Plastic Strains Following Full Transformation: Experiments Versus Micro-mechanical Simulations

7. CONCLUSION

In conclusion, this study has undertaken a thorough examination of the numerical implementation of Leblond *et al.*'s advanced model for phase transformation, with a specific focus on its application to critical thermo-mechanical processes such as welding and quenching. The investigation has been meticulous, centering on the precision and reliability of this implementation within finite element analysis and providing valuable insights into the complex interplay of thermal, metallurgical, and mechanical phenomena. Through the practical application of Leblond *et al.*'s model to predict phase transformation phenomena in A.508 cl and A533 steels, the research has effectively demonstrated the model's robustness and efficiency in delivering accurate numerical simulations of thermo-mechanical processes.

This work contributes significantly to the advancement of our understanding of material responses during phase transformations, offering enhanced predictive capabilities for computational tools in industrial applications. By showcasing the practical utility of the model in a specific steel context, the study not only validates its effectiveness but also provides a foundation for further refinement and application in diverse material scenarios. Overall, the findings presented here mark a valuable contribution to the field, paving the way for improved modeling and simulation techniques in the realm of thermo-mechanical processes and reinforcing the role of computational tools in advancing industrial practices.

References

[1] M. CORET, S. CALLOCH et A. COMBESCURE : Experimental study of the phase transformation plasticity of 16mnd5 low carbon steel under multiaxial loading. International Journal of plasticity, 18(12) :1707– 1727, 2002.

[2] M. CORET, S. CALLOCH et A. COMBESCURE : Experimental study of the phase transformation plasticity of 16mnd5 low carbon steel induced by proportional and nonproportional biaxial loading paths. European Journal of Mechanics-A/Solids, 23(5) :823–842, 2004.

[3] Y. DESALOS : Comportement mécanique et dilatométrique de lauténite métastable de l'acier A533, 1981.

[4] G. W. GREENWOOD et R. JOHNSON:The deformation of metals under small stresses during phase transformations. Proc. R. Soc. London, Ser. A.Mathematical and Physical Sciences, 283(1394) :403–422, 1965.

[5] Inoue, TKSMT and Nakano, M and Kubo, T and Matsumoto, S and Baba, H, High accuracy control of a proton synchrotron magnet power supply, IFAC Proceedings Volumes,volume=14 number=2,3137–3142, 1981, Elsevier

[6] INOUE et Z. WANG : Coupling between temperature, stress and metallic structures during phase transformation and the analysis of carburized quenching of a steel gear. In Computational Mechanics 86, p.691–696. Springer, 1986.

[7] J.B. Leblond, G. Mottet, J.C. Devaux (1989) A theoretical and numerical approach to the plastic behaviour of steels during phase transformations—I. Derivation of general relations, Journal of the Mechanics and Physics of Solids, Volume 34, Issue 4, 1986, Pages 395-409, ISSN 0022-5096

[8] J.B. Leblond, G. Mottet, J.C. Devaux, A theoretical and numerical approach to the plastic behaviour of steels during phase transformations—II. Study of classical plasticity for ideal-plastic phases, Journal of the Mechanics and Physics of Solids, Volume 34, Issue 4, 1986, Pages 411-432, ISSN 0022-5096

[9] C. L. MAGEE et H. W. PAXTON : Transformation kinetics, microplasticity and aging of martensite in fe-31 ni. Rap. tech., Carnegie Inst of tech Pittsburgh PA, 1966.

Appendix A. The Material Properties for the A508 cl Steel

The material properties for the A508 cl steel include the young modulus, thermal conductivity, Poisson ratio, yield limit, and hardening rate. These properties play crucial roles in determining the mechanical and thermal behavior of the steel alloy. These properties are summarized in the table below for each of the phase the steel is made of:

	phase α	phase γ
Young modulus (MPa)	182 000	182 000
Poison ratio	0.3	0.3
Yield limit (MPa)	950	145
Hardening rate	0	0
Thermal deformation	0	0.84%

Table A.1: The Material Properties for the A508 cl Steel

Appendix A. The Material Properties for the A533 steel

The material properties for the A533 steel include the young modulus, Poisson ratio, and yield limit. These properties play crucial roles in determining the mechanical of the steel alloy. These properties are summarized in the table below for each of the phase the steel is made of:

	phase α	phase γ
Young modulus (MPa)	182 000	182 000
Poison ratio	0.3	0.3
Yield limit (MPa)	950	145

Table A.2: The Material Properties for the A533 steel